Fabrication of Carbon-Nanotube-Forest Based Bolometer

B. D. Wood[1], J. S. Dyer[2], V. A. Thurgood[2], and T.-C. Shen[1]

[1]*Department of Physics, Utah State University, Logan, UT 84322, USA*
[2]*Space Dynamics Laboratory, North Logan, UT 84341, USA*

Abstract Due to the nearly-vertical alignment and the band structure of graphite, carbon nanotube forests could have near-unity emissivity which make them ideal candidates as the absorbers for radiometric devices. However, forest height, carbon nanotube density, and the presence of surface defects will affect the total reflectance and transmittance. With optimized growth conditions, a total reflectance of 0.003 and a transmittance of 0.001 has been achieved in the 2 μm - 16 μm spectral region. Fabrication of a suspended thermistor-type bolometer incorporating a carbon nanotube forest as the absorber is discussed.

Introduction

The purpose of a bolometer is to measure the amount of radiation being absorbed on its surface. Converting incoming radiation into thermal energy results in a temperature change within the thermistor. The change in temperature alters the material's electrical resistance which is detected by external electronics, giving a measure of the incident radiation intensity. Parameters that characterize the bolometer's performance include responsivity, noise, detectivity, and thermal response time.[1] Noise is primarily influenced by the operating temperature of the bolometer. Although room-temperature will increase the thermal/Johnson noise of the device and limit the minimum amount of radiation that can be detected, most of the applications on environmental monitoring are not compatible with cryogenic operation. Thermal response time is the time it takes for the temperature of the thermistor to reduce to $1/e$ when thermal radiation is removed instantaneously. The thermal response time is defined by the ratio of thermal capacitance to thermal conductance. Clearly, a low thermal capacitance and a high thermal conductance can reduce time constant which is important for imaging. Responsivity is the defined as the ratio of the output signal to the input power intensity. Detectivity is the normalized signal-to-noise ratio. To have high responsivity and detectivity, high temperature coefficient of resistance (THR) of the thermistor, low thermal capacitance, low thermal conductivity, low operational temperature, and high emissivity of the absorber are desirable. Clearly, some design compromise is needed depending on the application. Nevertheless, smaller thermal capacitance, high emissivity, and a high THR are needed to improve all performance factors.

Carbon nanotube (CNT) forests have been claimed as the blackest man-made materials.[2,3] The emissivity could be greater than 0.98 in the spectral range of 0.2-200 μm with almost no height or wavelength dependence.[2] Further, the spectrum of the reflectance of CNT forest is featureless comparing with other common black paints, which is very useful for many applications. (Figure 1) Carbon nanotube forests can be grown selectively on silicon dioxide patterns[4]. Since the undoped silicon has a reasonable THR as a thermistor in the ambient temperature range, combining with standard microfabrication techniques, suspended microscale silicon structures could provide an interesting system to study radiometry. There have been studies on the reflectance[5-10] and

absorption coefficient[11], but to the best of our knowledge, the CNT density effect has not been reported. Here we report our study of the optical properties of the CNT forests on various substrates. We find that the CNT density has a strong effect on the reflectance and transmittance of a forest in the mid-infrared range. Fabrication of the silicon bolometer is in progress.

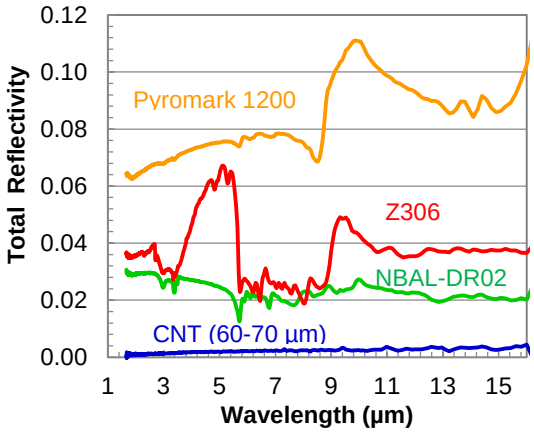

Fig. 1 *Total reflectance of a CNT forest of 60-70 µm in height comparing with those of black paints.*

Experimental

Carbon nanotube forests were grown using a chemical vapor deposition method. Growth temperature was set at 700 ^{o}C. The liquid precursor is a solution of ferrocene dissolved in xylene in various concentrations. The precursor was injected into the growth chamber by a syringe pump with a H_2:Ar=1:1 mixture as the carrier gas. As the precursor dissociates, iron atoms diffuse across and into the substrate and coalesce to form nanometer-scale catalyst particles which promote the dissociation of C-containing molecules to grow CNTs. Ideally, the catalyst particle will stay anchored to the substrate and supply C continuously for each CNT growth. However, the CNT growth will be terminated by various factors including reduced C supply due to increasing forest height and amorphous C deposition which inactivates the catalyst. It should be noted that the CNTs in a forest is not perfectly aligned. The entanglement increases light reflection and absorption as our data suggest. Furthermore, the CNT density in a forest decreases from tip to base, as a result of the inactivated CNT being lifted up by the growing neighbors from the entanglement.[12,13] The misalignment of CNT and density variation within a forest render the modeling of optical properties of the CNT forest a daunting task.

In addition to the ferrocene concentration in the precursor, substrates dictate the CNT density of a forest, depending on the Fe diffusion rate into the substrates. Insulators such as quartz, SiO_2 and Al_2O_3 act as a diffusion barrier for Fe so the catalyst particles can form easily while most metals and pure Si allow rapid Fe in-diffusion and, hence, do not substantiate CNT forest growth.

We have grown and studied CNT forests on 10x10 mm substrates of fused silica, sapphire, and Si coated with Al, Mo, and Nb. Total diffuse reflectance and transmittance data from 2 µm to 16 µm in wavelength were taken with a FTIR spectrometer using an integrating sphere accessory.

Results and discussion

1. CNT density effects on reflectance

Both sample A and B were 14-18 µm tall CNT forests grown on Al (3 nm)/Nb (66 nm) coated Si substrates. However, the precursor for A has 1.5 % ferrocene concentration while the precursor for B has only 0.5 % ferrocene concentration. As a result, the CNT density in A is visibly higher than that of B as shown in Fig. 2 (a) and2 (b). The random CNT forest pattern of 2(b) is caused by the slight difference in Nb/Si alloy formation at the growth temperature. Figure 2(c) shows that the total reflectance of A is significantly higher than that of B. However, if the CNT density is too low, the reflectance from the substrate can contribute to the total reflection. Sample C is a ~36-µm tall CNT forest grown on a fused silica substrate by a precursor

with ferrocene concentration of 1.5 %. Comparing with the Al/Nb/Si substrate, the CNT density on fused silica substrate is much less. As a result, the rays reflected from the substrate interfere with those from the forest top creating a fused silica peak near 9 µm as shown in the curve C of Fig. 2(c).

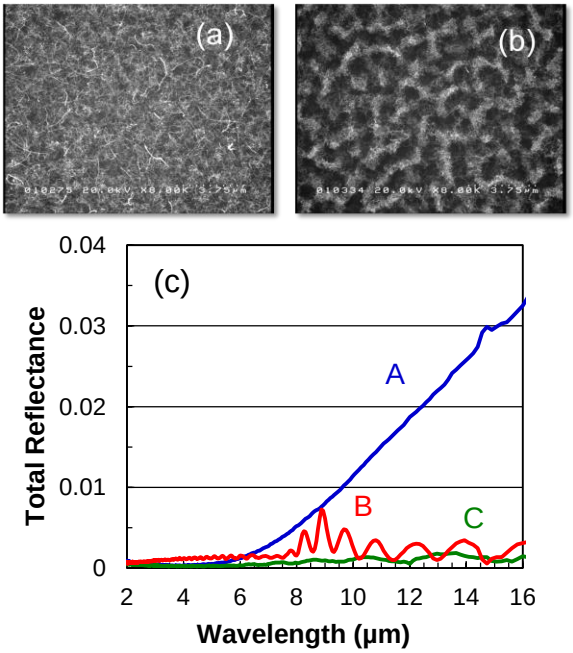

Fig. 2 *(a) Top view of CNT forest A by 1.5% ferrocene precursor. (b) Top view of CNT forest B by 0.5 % ferrocene precursor . (c) Total reflectance of A (blue), B (green) and C (red) which was grown by 1.5% ferrocene precursor on fused silica.*

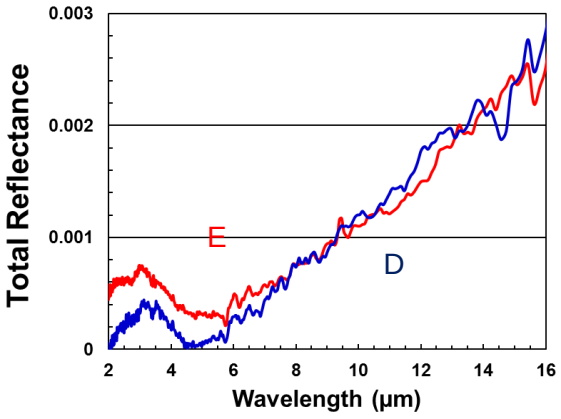

Fig. 3 *CNT forest of E (red) is about twice as tall as D (blue) but their CNT density is about the same.*

2. Forest height on reflectance

If the CNT density is low, forest height would increase the chance of the secondary reflection from the substrate to be absorbed, thus reducing the reflectance. Otherwise, the forest height should have little effect on the reflectance. The majority of the reflectance is caused by the misaligned crust layer on the CNT forest surface. Samples D and E have been grown by the same precursor of 0.5 % ferrocene concentration on 3-nm Al-coated Si substrates, but the height of E is ~50 µm, twice as high as D (~25 µm). As shown in Fig. 3, the total reflectance of both samples are quite similar.

3. Forest height effects on transmittance

Since the transmittance is the samples' ability to let radiation enter and escape the entire sample, a strong correlation between both the forest height and CNT density could be expected. Sample F and G were both prepared

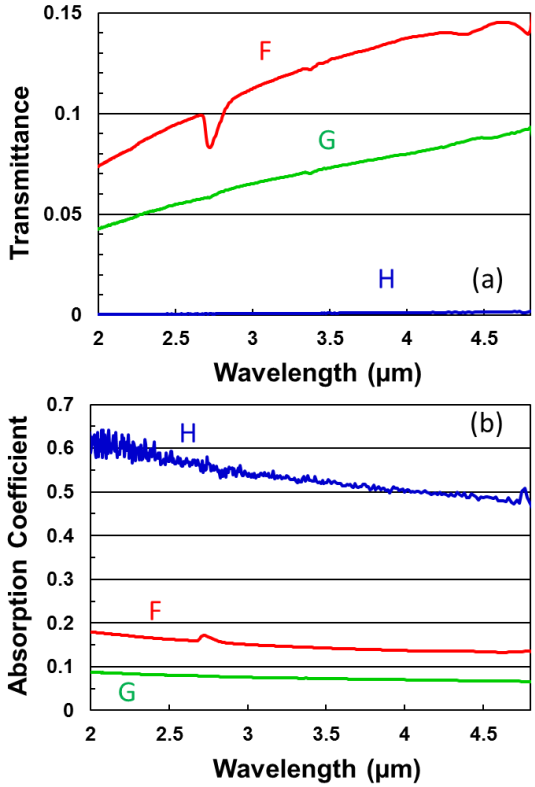

Fig. 4 *(a) Transmittance of sample F (red), G (green) and H (blue). (b) Absorption coefficient of F ,G and H.*

by a precursor of 1.5 % ferrocene concentration on fused silica substrate, but forest F is only 14.5 µm high while G is 36 µm high. As depicted in Fig. 4(a), the taller forest G (green) has much lower transmittance than the shorter forest F (red). Note that the transmittance of a CNT forest is obtained by dividing the raw transmission data by the transmission of a bare substrate. Because fused silica cannot transmit wavelengths longer than 4.8 µm, so we cannot measure the CNT forest transmittance at longer wavelengths on fused silica substrate.

4. CNT density effects on transmittance

Higher CNT density also increases radiation absorption. Forest H was grown on fused silica with a precursor of 3.0 % ferrocene concentration and the forest height is ~14 µm. As shown in Fig. 4(a), Forest H has very low transmittance even though the height is comparable to F.

The absorption coefficient α can be deduced via the expression

$$T_{Sample}(\lambda) = T_{Substrate}(\lambda)e^{-\alpha(\lambda)\cdot d}$$

where *d* is the average thickness of the sample and *T* is the transmittance. We note that the absorption coefficient is higher for the denser forest H. (Fig. 4b) The absorption coefficient increases toward shorter wavelengths. One would expect the absorption coefficient to be independent of the forest height. However, it is interesting to note that the absorption coefficient for the shorter forest F is higher than that for the longer forest G. We speculate that this can be attributed to the variation of CNT density in a forest throughout their height. A taller forest will have a larger fraction of its height at low density resulting in less absorption.

5. Emissivity

The emissivity is a parameter describing how well an object can radiate energy and is defined as the power radiated by an object normalized to that of an ideal black body and is a temperature dependent quantity.[10] If the temperature of the object stays relatively constant or if the temperature change happens quasi-statically, the total incident power can be divided into optical components

$$I_{inc.} = I_{Reflected} + I_{Transmitted} + I_{absorbed}$$

The intensity that gets absorbed will be converted into thermal energy, which dictates how much the object will emit radiation. Writing the intensities as percentages of the incident, the emissivity ε can be expressed as

$$\varepsilon = 1 - reflectance - transmittance.$$

Therefore, reflectance and transmittance need to be minimized the get the highest emissivity of the carbon nanotubes. Emissivity is the only property of the absorber that has influence on the efficiency of the bolometer.

6. Bolometer fabrication

To create a suspended Si thermistor as the heart of the bolometer, we will use standard microfabrication techniques on silicon-on-insulator (SOI) wafers. Using mask 1 (Fig. 5a) with a positive photoresist to define the contact and the thermistor. Once developed, the exposed oxide is removed by a buffered HF etch followed by a KOH etch to create a mesa for the thermistor and the contact area. After removing the oxide, mask 2 (Fig. 5b) will be used to create a 3-nm Al coating on the thermistor. Finally, mask 3 (Fig. 5c) will be used to create a Au coating on the contact

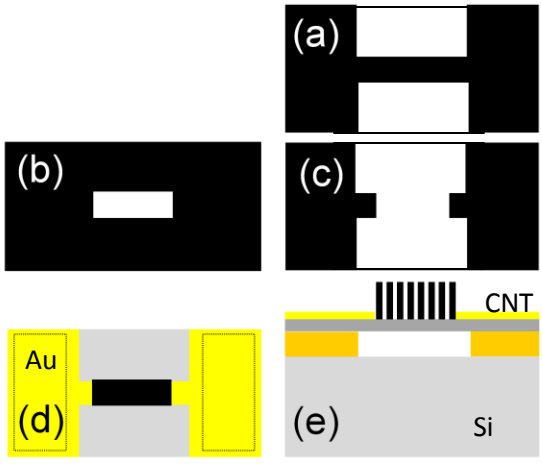

Fig. 5 *(a) mask 1 (b) Mask 2 (c) Mask 3 (d) Top view and (e) side view of the CNT bolometer.*

region. The finished Si structure will be moved to the CVD chamber to grow a CNT forest on the Al/Si region. The schematics of the top and side view of the finished bolometer are presented in Fig. 5d and 5e.

Conclusion

Reflectance and transmittance are two properties of CNT forests that are closely related to their morphology. The forest morphology can be controled with the precursor and should be fine tuned for every substrate. Surface defects can also affect the optical properties. Forest density has to be managed to get the lowest reflectance followed by a proper height to reduce the transmission. With an optimized morphology, a forest of 20-μm tall can yield a reflectance of less than 0.3 % and a total transmission of less than 0.1 %, allowing it to absorb 99.6% of the total radiation in the mid-IR spectrum. With a near perfect emissivity, we plan to explore the dimensions of the thermistor and the microbridges to optimize the thermal response time, detectivity, and responsivity of the bolometer.

Samples	Substrate	ferrocene (mol %)	Height (μm)
A	Al/Nb/Si	1.5	8.2-14
B	Al/Nb/Si	0.5	16.5-18.4
C	fused silica	1.5	32-40
D	Al/Si	0.5	24-27
E	Al/Si	0.5	42-51
F	fused silica	1.5	14.5
G	fused silica	1.5	32-40
H	fused silica	3.0	11-16.5

Table 1 *Substrate, ferrocene concentration, and CNT forest height of all the samples.*

Acknowledgements

This work was supported by Space Dynamics Laboratory. BDW would like to thank the fellowship of NASA EPSCoR Space Grant consortium.

References

1. Kosarev, A. Torres, M. Moreno, *Bolometers: Theory, Types and Applications,* New York, Nova Science Publishers, 1-57 (2011).
2. K. Mizuno, J. Ishii, H. Kishida, Y. Hayamizu, S. Yasuda, D. N. Futaba, M. Yumura, K. Hata, Proc. Nat. Acad. Sci. **106** 6044-47 (2009).
3. Z.-P. Yang, M.-L. Hsieh, J. A. Bur, L. Ci, L. M. Hanssen, B. Wilthan, P. M. Ajayan, S.-Y. Lin, Appl. Optics **50**, 1850 (2011).
4. Z. J. Zhang, B. Q. Wei, G. Ramanath, P. M. Ajayan, Appl. Phys. Lett. **77**, 3764 (2000).
5. T. d. l. Arcos, P. Oelhafen, D. Mathys, Nanotech. **18**, 265706 (2007).
6. M.A. Quijada, J.G. Hagopian, S. Getty, R.E. Kinzer, E.J. Woolack, Proc. SPIE **8150,** 815002-1 (2011).
7. H. Shi, J.G. Ok, H.W. Baac, L.J. Guo, AIP, **99**, 211103 (2011).
8. X.J. Wang, J.D. Flicker, B.J. Lee, W.J. Ready, Z.M. Zhang, Nanotech. **20**, 215704 (2009).
9. J.G. Hagopian, S.A. Getty, M. Quijada, J, Tveekrem, R. Shiri, P. Roman, J. Butler, G. Georgiev, J. Livas, C. Hunt, A. Maldonado, Proc. SPIE **7761,** 77610F-1 (2010).
10. M.A. Quijada, J.G. Hagopian, S. Getty, R.E. Kinzer, E.J. Wollack, Proc. SPIE **8150**, 815002 (2011.)
11. H. Ye, X.J. Wang, W. Lin, C.P. Wong, Z.M. Zhang, Appl. Phys. Lett. **101,**141909 (2009).
12. R. W. Call, C. G. Read, C. Mart, and T.-C. Shen, J. Appl. Phys. **112**, 124303 (2012).
13. M. Bedewy, E. R. Meshot, H. Guo, E. A. Verploegen, W. Lu, A. J. Hart, J. Phys. chem. C **113**, 20576 (2009).